PAPER

Check for updates

Methyl-restricted rotor rotation on the stator produces high-efficiency fluorescence emission: a new strategy to achieve aggregation-induced emission†

Haicheng Yang, [iD] Xinyue Zhou, Tianqi Hui, Yingying Han, Xiaonan Jiang and Jie Yan*

At present, we have realized that the aggregation-induced emission (AIE) achieves the purpose of fluorescence enhancement by restricting rotations to reduce intermolecular or intramolecular energy loss. Based on this idea, we synthesized a novel fluorene-based fluorescent compound with a restricted rotor rotation on the stator through the Suzuki coupling reaction. The luminescence effect was evaluated by comparing its fluorescence intensity with that of the control compound. Finally, theoretical calculations showed that the presence of methyl groups hindered the thermal rotation of the fluorenyl groups. Thus, the results indicated that the fluorescence of this compound was better than that of the control compound. A new synthetic pathway for high-efficiency AIE-based fluorescent luminogens has been developed.

Introduction

Aggregation-induced emission (AIE)[1] is a new phenomenon that is contrary to the commonly observed aggregation-caused quenching (ACQ).[2] Because of its important academic value and diversified applications in fluorescent sensors,[3–5] bioprobes,[6–8] optoelectronic devices,[9–11] and mechanical color-changing smart materials,[12–14] it has stimulated extensive research interest. Novel AIE nano-fluorescent probes have excellent water solubility,[15] biocompatibility and optical properties,[16,17] and can be applied in disease diagnosis, environmental detection, cell imaging and chemical sensors.[18,19] The most important one among these is the application in cell imaging. Fluorescent probes that are used to enter cells and image require a simple designs and surface functionalizations,[20] biodegradability and good biocompatibility. In order to achieve these functions, Wei *et al.* developed a series of small fluorescent molecules with the AIE effect, and also developed AIE fluorescent mesoporous silica nanoparticles for intracellular imaging.[21–23] Some functionalized fluorescent nanoparticles have demonstrated specific targeting ability towards cancer cells, which is used for therapeutic diagnosis, and significant progress has been made.[24,25] Recently, Tang *et al.* reported a series of triphenylamine (TPA)–thiophene building block-based AIEgens having tunable maximum emission

wavelengths covering the visible and NIR regions for cell imaging. The emission colors were tuned by simple alteration of the HOMO–LUMO energy levels by the introduction of electron donor (D)–acceptor (A) substituents.[26]

A large amount of research has been devoted to the basic understanding of the mechanism behind the AIE phenomenon,[27–31] both to solve ACQ and develop efficient solid state luminogens. Theoretical calculations and experimental results have suggested that the restriction of intramolecular rotation (RIR)[32,33] is the main cause of the AIE effect. In the solution state, the aromatic rotor typically annihilates the excitons in a nonradiative transition mode. However, in the aggregated state, the rotation of the rotor is restricted, resulting in the predominant radiative transition of the excited state, thus successfully producing luminogens.[34] Therefore, aromatic rotors are very important in the design of AIE active luminogens. It has been reported that the volume of the aromatic rotor,[35] the number of restricted benzene rings,[36] and the connection between the stator and the rotor[37] all affect the luminous efficiency of the AIE light-emitting device. However, there are few reports of groups on the stator that restrict the rotation of the fluorescent rotor. The beneficial outcome of the AIE effect would be to restrict the rotation of the rotor in the aggregated state, reduce the non-radiative annihilation process, and promote the radiative quenching pathway. Therefore, the rotation of the rotor is restricted, and the plane π-conjugate is better generated between the rotor and the stator, which can increase the luminogens emission efficiency to some extent. In order to gain a deeper understanding of the relationship between the structure of AIE luminescent materials and the

College of Chemistry and Chemical Engineering, Liaoning Normal University, Huanghe Road 850#, Dalian City, 116029, PR China. E-mail: yhc1994@live.cn

† Electronic supplementary information (ESI) available: ¹H and ¹³C NMR spectra and additional figures. See DOI: 10.1039/c9ra01636h

intensity of luminescence, we have focused on fluorene-substituted methylbenzene, an AIE luminescent agent with a twisted propeller conformation with a large sterically hindered stator.

We want to know if the fluorescence of the AIE luminogens can be enhanced to some extent when a large sterically hindered group blocks the aromatic rotor. For this, we prepared a new large sterically hindered fluorene-substituted methylbenzene (1,3,5-tris(9,9-dimethylfluoren-2-yl)-2,4,6-trimethylbenzene) (TFTB) and compared its luminescence properties with fluorene-substituted benzene without large sterically hindered groups (1,3,5-tris(9,9-dimethylfluoren-2-yl)benzene)[38,39] (TFB) (Chart 1).

Experimental

Chemicals and instruments

Mesitylene, 2-bromo-9,9-dimethylfluorene and all other chemicals and reagents were purchased from Aladdin Industrial Corporation. THF was distilled under dry nitrogen immediately prior to use. ^{1}H and ^{13}C NMR spectra were measured on a Bruker AV 500 spectrometer in deuterated chloroform or dichloromethane using tetramethylsilane (TMS; $\delta = 0$) as the internal reference. UV-Vis spectra were measured on a JASCO V-570 spectrophotometer. Photoluminescence was recorded on a JASCO FP-6500 spectrophotometer. Thermal transitions were investigated by differential scanning calorimetry using a STA 449 F3 under dry nitrogen at a heating rate of $10\,^\circ\text{C min}^{-1}$. High resolution mass spectrometry was measured on a LTQ-Orbitrap XL high resolution mass spectrometer. X-ray diffraction patterns were recorded on a D8 Advance powder diffractometer using the monochromatized X-ray beam from a nickel-filtered Cu Kα radiation ($\lambda = 1.54183$ Å).

Aggregation-induced emission investigation

Stock THF solutions of the luminogens with a concentration of 100 μM were prepared. Aliquots of the stock solution were transferred to 10 mL volumetric flasks. After appropriate amounts of THF were added, water was added dropwise under vigorous stirring to furnish 10 μM solutions with different water contents. The PL measurements of the resultant solutions were then performed immediately.

Synthetic details

Procedure for the synthesis of 1. A mixture of mesitylene (6.0 g, 50 mmol), I_2 (15.5 g, 60 mmol), $HIO_4\cdot 2H_2O$ (7.0 g, 32.5 mmol), and H_2SO_4 (3 mL) in acetic acid (50 mL)–water (10 mL) was stirred at 90 °C for 10 h. The reaction mixture was diluted with water (125 mL), and the resulting precipitate was filtered, washed with water to remove the acid, and washed with acetone to give 1,3,5-triiodo-2,4,6-trimethylbenzene, a white solid (21.0 g, 84.5%). ^{1}H NMR (500 MHz, $CDCl_3$), δ (TMS, ppm): 3.01 (s 9H). ^{13}C NMR (125 MHz, $CDCl_3$), δ (TMS, ppm): 144.15, 101.16, 39.56.

Procedure for the synthesis of 2. A mixture of 1,3,5-triiodo-2,4,6-trimethylbenzene (3.0 g, 6.03 mmol), 4,4,4′,4′,5,5,5′,5′-octamethyl-2,2′-bi(1,3,2-dioxaborolane) (6.3 g, 25.86 mmol), $PdCl_2(dppf)$ (0.2 g), and KOAc (4.0 g, 29.5 mmol) was added to a flask. The flask was connected to a Schlenk line, which evacuated the air and refilled the flask with nitrogen. Then, 50 mL of DMF was degassed and added through a cannula. The flask was equipped with a water condenser and stirred at 90 °C under nitrogen for 24 h. After cooling to room temperature, 25 mL of water was added and then extracted with CH_2Cl_2 (3 × 50 mL); the combined organic layer was washed with saturated saline and dried over anhydrous $MgSO_4$. The solvent was evaporated and the residue was purified by column chromatography over silica gel using ethyl acetate/petroleum ether (1 : 4, v/v); then, it was recrystallized from hexane to give 1,3,5-tris(4,4,5,5-tetramethyl-1,3,2-dioxaborolan-2-yl)-2,4,6-trimethylbenzene, which was a colorless transparent solid (2.40 g, 80%). ^{1}H NMR (500 MHz, $CDCl_3$), δ (TMS, ppm): 2.39 (s, 9H), 1.34 (s, 36H). ^{13}C NMR (125 MHz, $CDCl_3$), δ (TMS, ppm): 147.02, 84.71, 26.38, 23.99. HRMS: m/z 498.3495 (M$^+$, calcd 498.0756).

Procedure for the synthesis of 3 (TFTB) (pathway c). A mixture of 1,3,5-tris(4,4,5,5-tetramethyl-1,3,2-dioxaborolan-2-
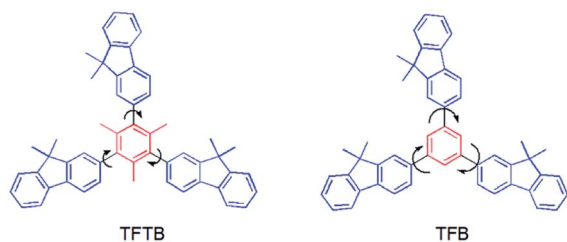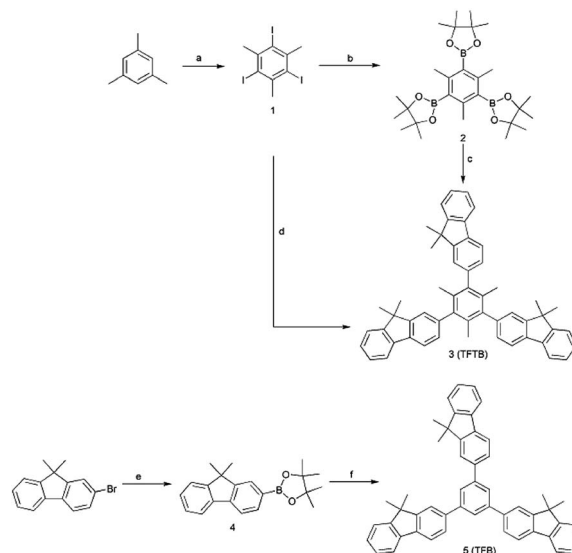

Scheme 1 Reactions and conditions: (a) $HIO_4\cdot 2H_2O$, I_2, H_2SO_4, acetic acid, water; (b) 4,4,4′,4′,5,5,5′,5′-octamethyl-2,2′-bi(1,3,2-dioxaborolane), $PdCl_2(dppf)$, KOAc, DMF; (c) 2-bromo-9,9-dimethylfluorene, Pd(PPh$_3$)$_4$, K$_3$PO$_4$, DMSO, water; (d) 2-(9,9-dimethylfluoren-2-yl)-4,4,5,5-tetramethyl-1,3,2-dioxaborolane, Pd(PPh$_3$)$_4$, K$_3$PO$_4$, dioxane, water; (e) 4,4,4′,4′,5,5,5′,5′-octamethyl-2,2′-bi(1,3,2-dioxaborolane), $PdCl_2(dppf)$, KOAc, DMF; (f) 1,3,5-tribromobenzene, Pd(PPh$_3$)$_4$, K$_3$PO$_4$, dioxane, water.

Chart 1 AIE luminogen TFTB and its control example.

yl)-2,4,6-trimethylbenzene (1.0 g, 2.0 mmol), 2-bromo-9,9-dimethylfluorene (1.9 g, 6.96 mmol), Pd(PPh$_3$)$_4$ (0.2 g, 17 mmol), and K$_3$PO$_4$ (3.0 g, 14.17 mmol) was added to a flask. The flask was connected to a Schlenk line, which evacuated the air and refilled the flask with nitrogen. A solution of 30 mL of DMSO and 2 mL of water was degassed and added through a cannula. The flask was equipped with a water condenser and stirred at 95 °C under nitrogen for 48 h. After cooling to room temperature, 25 mL of water was added and then extracted with CH$_2$Cl$_2$ (3 × 50 mL); the combined organic layer was washed with saturated saline and dried over anhydrous MgSO$_4$. The solvent was evaporated and the residue was purified by column chromatography over silica gel using CH$_2$Cl$_2$/petroleum ether (1 : 5, v/v); then, the solvent was removed to give 1,3,5-tris(9,9-dimethylfluoren-2-yl)-2,4,6-trimethylbenzene (TFTB), a white solid (0.21 g, 14%).

Procedure for the synthesis of 3 (TFTB) (pathway d). A mixture of 1,3,5-triiodo-2,4,6-trimethylbenzene (1.0 g, 2.01 mmol), 2-(9,9-dimethylfluoren-2-yl)-4,4,5,5-tetramethyl-1,3,2-dioxaborolane (2.56 g, 8.0 mmol), Pd(PPh$_3$)$_4$ (0.2 g, 17 mmol), and K$_3$PO$_4$ (3.0 g, 14.17 mmol) was added to a flask. The flask was connected to a Schlenk line, which evacuated the air and refilled the flask with nitrogen. A solution of 30 mL of dioxane and 2 mL water was degassed and added through a cannula. The flask was equipped with a water condenser and stirred at 85 °C under nitrogen for 24 h. After cooling to room temperature, 25 mL of water was added and then extracted with CH$_2$Cl$_2$ (3 × 50 mL); the combined organic layer was washed with saturated saline and dried over anhydrous MgSO$_4$. The solvent was evaporated and the residue was purified by column chromatography over silica gel using CH$_2$Cl$_2$/petroleum ether (1 : 5, v/v); then, the solvent was removed to give 1,3,5-tris(9,9-dimethylfluoren-2-yl)-2,4,6-trimethylbenzene (TFTB), a white solid (0.71 g, 51%). ^{1}H NMR (500 MHz, CDCl$_3$), δ (TMS, ppm): 7.79 (d, J = 7.8 Hz, 3H), 7.75 (d, J = 6.7 Hz, 3H), 7.69 (d, J = 1.4 Hz, 3H), 7.63 (dd, J = 7.8, 1.7 Hz, 3H), 7.45 (d, J = 6.3 Hz, 3H), 7.37–7.30 (m, 6H), 3.00 (s, 9H), 1.56 (s, 18H). ^{13}C NMR (125 MHz, CDCl$_3$), δ (TMS, ppm): 155.73, 155.35, 145.57, 142.28, 140.35, 139.82, 128.66, 128.46, 127.73, 124.04, 122.84, 121.71, 121.49, 102.60, 48.42, 40.98, 28.72. HRMS: m/z 696.3756 (M$^+$, calcd 696.9589).

Procedure for the synthesis of 4. A mixture of 2-bromo-9,9-dimethylfluorene (5.0 g, 18.31 mmol), 4,4,4′,4′,5,5,5′,5′-octamethyl-2,2′-bi(1,3,2-dioxaborolane) (4.8 g, 19 mmol), PdCl$_2$(dppf) (0.2 g), and KOAc (4.0 g, 29.5 mmol) was added to a flask. The flask was connected to a Schlenk line, which evacuated the air and refilled the flask with nitrogen. 50 mL of DMF was degassed and added through a cannula. The flask was equipped with a water condenser and stirred at 100 °C under nitrogen for 24 h. After cooling to room temperature, 25 mL of water was added and then extracted with CH$_2$Cl$_2$ (3 × 50 mL); the combined organic layer was washed with saturated saline and dried over anhydrous MgSO$_4$. The solvent was evaporated and the residue was purified by column chromatography over silica gel using CH$_2$Cl$_2$/petroleum ether (1 : 20, v/v); then, it was recrystallized from hexane to give 2-(9,9-dimethylfluoren-2-yl)-4,4,5,5-tetramethyl-1,3,2-dioxaborolane, a colorless

transparent solid (4.40 g, 75%). ^{1}H NMR (500 MHz, CDCl$_3$), δ (TMS, ppm): 7.88 (s, 1H), 7.81 (d, J = 7.5 Hz, 1H), 7.74 (dd, J = 12.1, 5.7 Hz, 2H), 7.45–7.41 (m, 1H), 7.35–7.30 (m, 2H), 1.50 (s, 6H), 1.38 (s, 12H). ^{13}C NMR (125 MHz, CDCl$_3$), δ (TMS, ppm): 154.32, 154.12, 153.70, 152.77, 142.21, 141.27, 140.39, 139.20, 138.99, 137.48, 133.49, 128.77, 128.08, 127.75, 126.97, 123.82, 122.64, 120.44, 119.88, 119.34, 83.75, 46.87, 27.08, 24.93, 19.62.

Procedure for the synthesis of 5. A mixture of 1,3,5-tribromobenzene (1.0 g, 3.18 mmol), 2-(9,9-dimethylfluoren-2-yl)-4,4,5,5-tetramethyl-1,3,2-dioxaborolane (3.1 g, 9.68 mmol), Pd(PPh$_3$)$_4$ (0.2 g), and K$_3$PO$_4$ (3.0 g, 14.17 mmol) was added to a flask. The flask was connected to a Schlenk line, which evacuated the air and refilled the flask with nitrogen. A solution of 30 mL of dioxane and 2 mL of water was degassed and added through a cannula. The flask was equipped with a water condenser and stirred at 85 °C under nitrogen for 24 h. After cooling to room temperature, 25 mL of water was added and then extracted with CH$_2$Cl$_2$ (3 × 50 mL); the combined organic layer was washed with saturated saline and dried over anhydrous MgSO$_4$. The solvent was evaporated and the residue was purified by column chromatography over silica gel using CH$_2$Cl$_2$/petroleum ether (1 : 5, v/v); then, the solvent was removed to give 1,3,5-tris(9,9-dimethylfluoren-2-yl)benzene (TFB), a white solid (1.52 g, 73%). ^{1}H NMR (500 MHz, CDCl$_3$), δ (TMS, ppm): 7.89 (s, 3H), 7.85 (d, J = 7.8 Hz, 3H), 7.78 (dd, J = 6.3, 1.2 Hz, 6H), 7.73 (dd, J = 7.8, 1.6 Hz, 3H), 7.47 (dd, J = 6.3, 1.2 Hz, 3H), 7.39–7.32 (m, 6H), 1.57 (s, 18H). ^{13}C NMR (125 MHz, CDCl$_3$), δ (TMS, ppm): 154.42, 153.97, 142.97, 140.55, 138.84, 127.37, 127.08, 126.54, 125.37, 122.66, 121.78, 120.38, 120.15, 47.07, 27.29. HRMS: m/z 654.3287 (M$^+$, calcd 654.8792).

Results and discussion

Synthetic strategy

The compound TFTB was prepared by a Suzuki coupling reaction,[40] which was carried out using an aryl boronate in the presence of a base and a Pd (0) catalyst (Scheme 1). The first synthesized 1,3,5-tris(4,4,5,5-tetramethyl-1,3,2-dioxaborolan-2-yl)-2,4,6-trimethylbenzene and 2-bromo-9,9-dimethylfluorene can be used as the substrate.[41–43] It is also possible to use 1,3,5-triiodo-2,4,6-trimethylbenzene and 2-(9,9-dimethylfluoren-2-yl)-4,4,5,5-tetramethyl-1,3,2-dioxaborolane as substrates, and the target compounds can be obtained by both methods. However, the second method resulted in a higher yield (51%) due to the steric hindrance of the reaction. Their spectra can be found in the ESI.† Its powder was crystalline, as revealed by the X-ray diffractogram (Fig. S1†). All luminescent agents are soluble in common organic solvents such as tetrahydrofuran (THF), but insoluble in water.

Aggregation-induced emission (AIE) property

To test if TFTB is AIE active, we added water to its THF solution and recorded its PL spectrum in the water-THF mixture (Fig. 1). When the water fraction (f_w, vol%) in the water–THF mixture was less than 50%, its PL emission remained in a very weak state with only a slight change. When a large amount of water
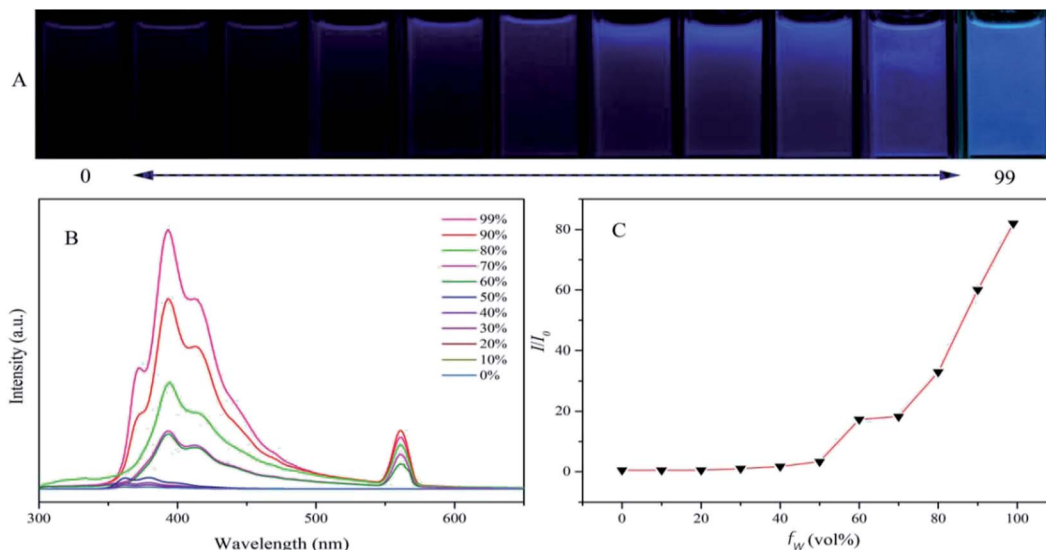
Fig. 1 (A) Photograph of TFTB in a water–THF mixed solution ($f_w = 0$–99%) under a UV lamp. (B) PL spectrum of TFTB in different fractions of water–THF mixed solution. (C) Fluorescence change pattern of TFTB in a water–THF mixed solution. (I_0 is the PL intensity in a pure THF solution.)

($f_w \geq 60\%$) was added, a long-wavelength emission with a peak at 394 nm appeared, and the intensity was greatly enhanced. The emission peak red-shifted compared to that of its THF solution and the frequency-doubled peak appeared at 561 nm. TFTB is insoluble in water, and an increase in water content causes the TFTB molecules to assume an aggregated state. The formation of aggregates greatly weakens the intramolecular rotation (IMR) process, causing the luminogens to emit intense fluorescence. A similar emission behavior of TFB was also observed in the water–THF mixture (Fig. S2†), confirming that it is also AIE active.

Computational research, photophysical properties

The molecular conformation was optimized by the semi-empirical PM3 method (Fig. 2). The fluorene unit was
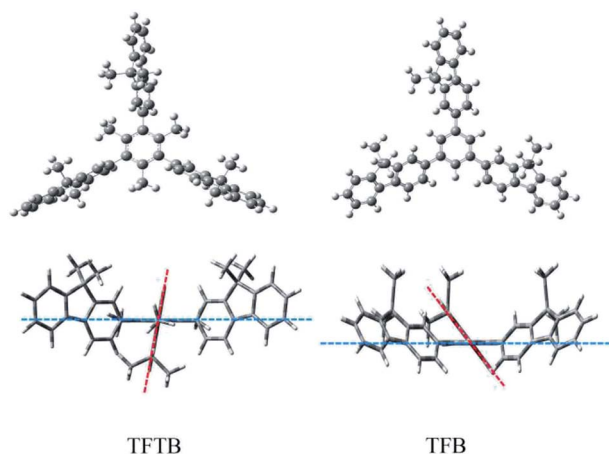
arranged in a star-shaped propeller shape. The highly twisted conformation of the TFTB results in a poor electronic communication between the rotor and the stator and little orbital overlap. Molecular orbital amplitude maps of the LUMO and HOMO levels of the two molecules (Fig. S3†) show that they were clearly dominated by the orbits of the fluorene rings of the surrounding rotors. This indicates that the emission of TFTB is derived from the excited state of the rotor fluorene ring around it. Among them, the three fluorene rings of TFTB contribute to the LUMO and HOMO energy levels. However, there is a ring that does not contribute to its HOMO level at all in TFB.

TFTB shows the maximum absorption at 328 nm (Fig. S4†), and its energy band gap is calculated to be 4.77 eV (Fig. S5†). TFB shows the maximum absorption at 336 nm, and its energy band gap is calculated to be 4.32 eV. Since there is a fluorene ring in TFB that does not contribute to its HOMO level, this is also the reason why the energy band gap of TFTB is wider than that of TFB. This is in good agreement with the blue-shift of the absorption spectrum of TFTB in the THF solution. The structural difference between TFTB and TFB is that the former has three methyl groups on the stator. Following our hypothesis, it is clear that the hindrance of these three methyl groups restricts the rotation of the rotor, so that TFTB emits in the solution state, while TFB has only weak luminescence in the solution state. The gradually thickened TFTB and TFB in the THF solution (from 1 μM to 100 μM) only increase their emission intensities, and hardly affect their spectral distribution and peak position. TFTB has two peaks at 362 nm and 380 nm, while TFB has only one peak, which appears at 368 nm (Fig. 3). This is because the methyl group inside the TFTB molecule in the solution state hinders the IMR process of its luminescent rotor, causing its various portions to emit characteristic peaks. However, due to the IMR process, TFB loses energy between the rotor and the stator; the exciton radiation is attenuated, and the emission peaks of each part are mixed.
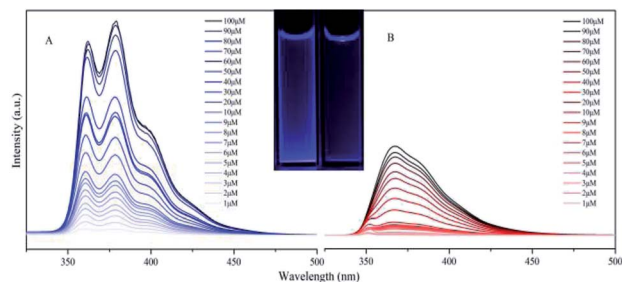

Fig. 2 Optimized molecular structures of TFTB and TFB calculated by a semi-empirical PM3 method. (The blue line represents the benzene ring plane; the red line represents the fluorene ring plane.)

Fig. 3 (A) PL spectra of different concentrations of TFTB in THF solution. (B) PL spectra of different concentrations of TFB in THF solution. (Intermediate panel) photograph of TFTB and TFB at the same concentration (1000 μM) in a THF solution under a UV lamp.

TFTB and TFB can also fluoresce in the solid state (Fig. 4A and C). Their solids show PL emission characteristics. The PL spectrum of the TFTB solid exhibits a peak at 424 nm (Fig. 4B). Its quantum yield is 37.44%. Its solid has very good fluorescence under UV light. The PL spectrum of the TFB solid exhibits a peak at 380 nm. Its quantum yield is 21.36%. However, the fluorescence of the solid under UV light is inferior to that of TFTB because the twisted conformation of TFTB makes it less prone to π-stacking. The TFB's fluorene rings can partially overlap in the solid state, resulting in strong intermolecular interactions, thereby reducing the emission efficiency. This is also confirmed from the $T_g = 328\ °C$ of TFB, which is greater than the $T_g = 282\ °C$ of TFTB (Fig. S6†), indicating that the TFB intermolecular interaction is stronger than TFTB. The above evidence demonstrates that restricting the intramolecular rotation can produce strong fluorescence emissions.

Potential energy surface scan

To further verify that the presence of methyl groups on the stator does hinder the rotation of the rotor, we calculated the total energy of the two molecular systems as a function of the angle between the fluorene ring plane and the benzene ring plane, as shown in the potential energy surface scan (Fig. 5). When the angle between the fluorene ring plane and the benzene ring plane of TFTB was 99.76°, the total energy of the entire molecular system was the lowest. When the angle was 189.76°, the fluorene ring was closest to the methyl group, and the total energy of the entire molecular system was the highest. When the TFB's fluorene-benzene dihedral angle was −38.03°, the total energy of the system was the lowest. When the angle was 81.97°, the total energy of the system was the highest. When both energies were highest, the energy of TFTB was much larger than that of TFB. However, after one revolution, the total energy of the TFTB system was not the same as the initial energy because the fluorene ring itself did not have a symmetrical structure. The methyl group was not evenly extruded on the fluorene ring. This is not the case with TFB. Collectively, these results verified that the methyl group on the stator could restrict the rotation of the rotor.
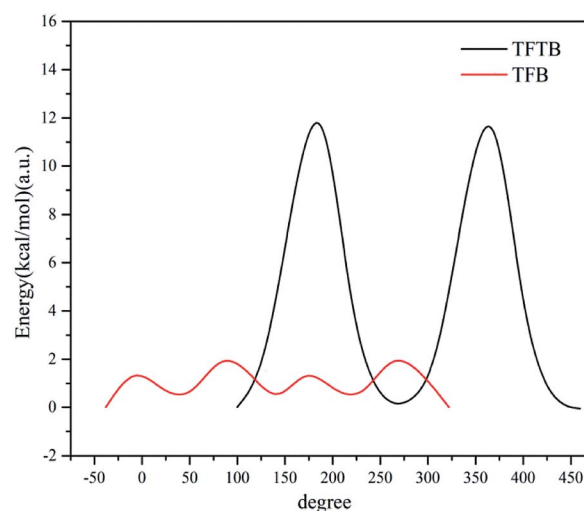

Fig. 5 The total energy of the system varies with the angle between the fluorene ring plane and the benzene ring plane.
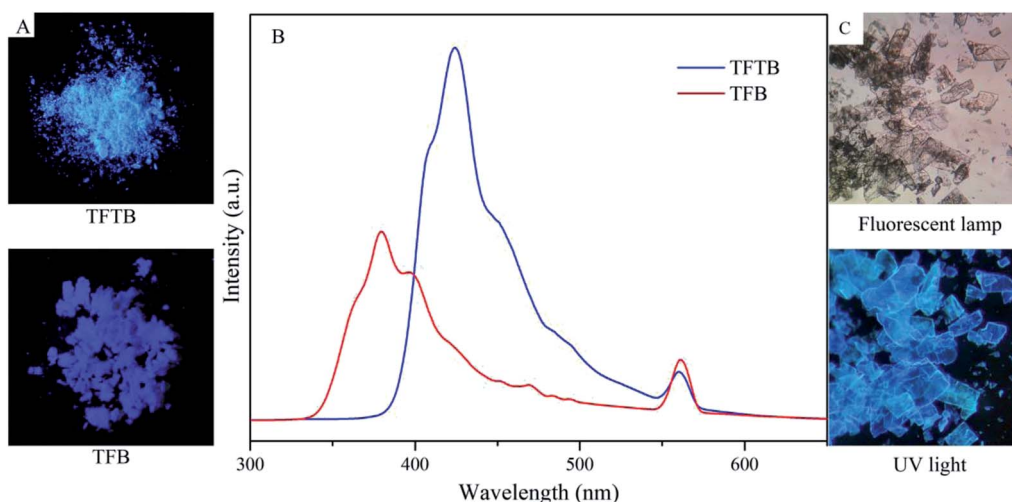

Fig. 4 (A) Photos of the solid under UV light. (B) Solid PL spectra of TFTB and TFB. (C) Photomicrograph of the TFTB solid.

Conclusions

In summary, a new AIE-active large sterically hindered fluorene-benzene copolymer TFTB and a new phenyl boronate intermediate were synthesized. By comparing the fluorescence properties of TFTB with those of the control compound TFB and from the theoretical calculation data, it was confirmed that the groups present on the stator could hinder the rotation of the fluorescent rotor and deactivate the IMR process, enhancing the fluorescence emission in solids and solutions. The properties of TFTB examined in this work provide a new strategy for synthesizing AIE luminogens with a distorted conformation.

Conflicts of interest

There are no conflicts to declare.

Acknowledgements

Notes and references

1 Y. Hong, J. W. Y. Lam and B. Z. Tang, *Chem. Commun.*, 2009, **0**, 4332.

2 Y. Hong, J. W. Y. Lam and B. Z. Tang, *Chem. Soc. Rev.*, 2011, **40**, 5361.

3 C. L. Tao, B. Chen, X. G. Liu, L. J. Zhou, X. L. Zhu, J. Cao, Z. G. Gu, Z. J. Zhao, L. Shena and B. Z. Tang, *Chem. Commun.*, 2017, **53**, 9975.

4 Z. M. Wang, F. Zhou, C. Gui, J. Wang, Z. J. Zhao, A. J. Qina and B. Z. Tang, *J. Mater. Chem. C*, 2018, **6**, 11261.

5 Z. Zhao, J. W. Y. Lam and B. Z. Tang, *J. Mater. Chem.*, 2012, **22**, 23726.

6 T. T. Kong, Z. Zhao, Y. Li, F. Wu, T. Jin and B. Z. Tang, *J. Mater. Chem. B*, 2018, **6**, 5986.

7 Y. L. Wang, C. Fan, B. Xin, J. P. Zhang, T. Luo, Z. Q. Chen, Q. Y. Zhou, Q. Yu, X. N. Li, Z. L. Huang, C. Li, M. Q. Zhu and B. Z. Tang, *Mater. Chem. Front.*, 2018, **2**, 1554.

8 J. Yang, J. Huang, Q. Li and Z. Li, *J. Mater. Chem. C*, 2016, **4**, 2663.

9 A. C. Sedgwick, L. L. Wu, H. H. Han, S. D. Bull, X. P. He, T. D. James, J. L. Sessler, B. Z. Tang, H. Tian and J. Yoon, *Chem. Soc. Rev.*, 2018, **47**, 8842.

10 W. W. H. Lee, Z. Zhao, Y. J. Cai, Z. Xu, Y. Yu, Y. Xiong, R. T. K. Kwok, Y. Chen, N. L. C. Leung, D. Ma, J. W. Y. Lam, A. J. Qin and B. Z. Tang, *Chem. Sci.*, 2018, **9**, 6118.

11 D. Ding, K. Li, B. Liu and B. Z. Tang, *Acc. Chem. Res.*, 2013, **46**, 2441.

12 Z. Zhuang, P. C. Shen, S. Y. Ding, W. W. Luo, B. R. He, H. Nie, B. H. Wang, T. B. Huang, R. R. Hu, A. J. Qin, Z. J. Zhao and B. Z. Tang, *Chem. Commun.*, 2016, **52**, 10842.

13 J. Liang, B. Z. Tang and B. Liu, *Chem. Soc. Rev.*, 2015, **44**, 2798.

14 X. Zhang, X. Zhang, L. Tao, Z. Chi, J. Xu and Y. Wei, *J. Mater. Chem. B*, 2014, **2**, 4398.

15 J. Z. Liu, J. W. Y. Lam and B. Z. Tang, *Chem. Rev.*, 2009, **109**, 5799.

16 Q. Wan, Q. Huang, M. Y. Liu, D. Z. Xu, H. Y. Huang, X. Y. Zhang and Y. Wei, *Appl. Mater. Today*, 2019, **9**, 145.

17 X. Y. Zhang, K. Wang, M. Y. Liu, X. Q. Zhang, L. Tao, Y. W. Chen and Y. Wei, *Nanoscale*, 2015, **7**, 11486.

18 X. Y. Zhang, X. Q. Zhang, B. Yang, M. Y. Liu, W. Y. Liu, Y. W. Chen and Y. Wei, *Polym. Chem.*, 2014, **5**, 356.

19 X. Y. Zhang, X. Q. Zhang, B. Yang, M. Y. Liu, W. Y. Liu, Y. W. Chen and Y. Wei, *Polym. Chem.*, 2014, **5**, 399.

20 Z. Long, M. Y. Liu, R. M. Jiang, Q. Wan, L. C. Mao, Y. Q. Wan, F. J. Deng, X. Y. Zhang and Y. Wei, *Chem. Eng. J.*, 2016, **308**, 527.

21 Z. Long, L. C. Mao, M. Y. Liu, Q. Wan, Y. Q. Wan, X. Y. Zhang and Y. Wei, *Polym. Chem.*, 2017, **8**, 5644.

22 Z. Long, M. Y. Liu, K. Wang, F. J. Deng, D. Z. Xu, L. J. Liu, Y. Q. Wan, X. Y. Zhang and Y. Wei, *Mater. Sci. Eng. C*, 2016, **66**, 215.

23 L. Huang, S. J. Yang, J. Y. Chen, J. W. Tian, Q. Huang, H. Y. Huang, Y. Q. Wen, F. J. Deng, X. Y. Zhang and Y. Wei, *Mater. Sci. Eng., C*, 2018, **94**, 270.

24 R. M. Jiang, M. Y. Liu, H. Y. Huang, L. C. Mao, Q. Huang, Y. Q. Wen, Q. Y. Cao, J. W. Tian, X. Y. Zhang and Y. Wei, *J. Colloid Interface Sci.*, 2018, **519**, 137.

25 J. Y. Chen, M. Y. Liu, Q. Huang, L. Huang, H. Y. Huang, F. J. Deng, Y. Q. Wen, J. W. Tian, X. Y. Zhang and Y. Wei, *Chem. Eng. J.*, 2018, **337**, 82.

26 W. H. Xu, M. M. S. Lee, Z. H. Zhang, H. H. Y. Sung, L. D. Williams, R. T. K. Kwok, J. W. Y. Lam, D. Wang and B. Z. Tang, *Chem. Sci.*, 2019, **10**, 3494.

27 J. Mei, N. Leung, R. Kwok, J. W. Y. Lam and B. Z. Tang, *Chem. Rev.*, 2015, **115**, 11718.

28 J. Mei, Y. Hong, J. W. Y. Lam, A. Qin, Y. Tang and B. Z. Tang, *Adv. Mater.*, 2014, **26**, 5429.

29 N. L. Leung, N. Xie, W. Yuan, Y. Liu, Q. Wu, Q. Peng, Q. Miao, J. W. Y. Lam and B. Z. Tang, *Chem.–Eur. J.*, 2014, **20**, 15349.

30 F. Bu, E. Wang, Q. Peng, R. Hu, A. Qin, Z. Zhao and B. Z. Tang, *Chem.–Eur. J.*, 2015, **21**, 4440.

31 H. Nie, K. Hu, Y. J. Cai, Q. Peng, Z. J. Zhao, R. R. Hu, J. W. Chen, S. J. Su, A. J. Qin and B. Z. Tang, *Mater. Chem. Front.*, 2017, **1**, 1125.

32 J. J. Guo, S. M. Hu, W. W. Luo, R. R. Hu, A. J. Qin, Z. J. Zhao and B. Z. Tang, *Chem. Commun.*, 2017, **53**, 1463.

33 H. T. Feng, Y. X. Yuan, J. B. Xiong, Y. S. Zheng and B. Z. Tang, *Chem. Soc. Rev.*, 2018, **47**, 7452.

34 J. Zhou, Z. F. Chang, Y. B. Jiang, B. R. He, M. Du, P. Lu, Y. N. Hong, H. S. Kwok, A. J. Qin, H. Y. Qiu, Z. J. Zhao and B. Z. Tang, *Chem. Commun.*, 2013, **49**, 2491.

35 J. Q. Shi, N. Chang, C. H. Li, J. Mei, C. M. Deng, X. L. Luo, Z. P. Liu, Z. S. Bo, Y. Q. Dong and B. Z. Tang, *Chem. Commun.*, 2012, **48**, 10675.

36 Z. Y. Yang, Z. H. Chi, Z. Mao, Y. Zhang, S. W. Liu, J. Zhao, M. P. Aldred and Z. G. Chi, *Mater. Chem. Front.*, 2018, **2**, 861–890.

37 X. H. Zhou, J. C. Yan and J. Pei, *Org. Lett.*, 2003, **5**, 3543.
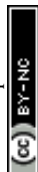
38 K. Okumoto and Y. Shirota, *Chem. Mater.*, 2003, **15**, 699.

39 B. Wang, X. L. Lv, D. W. Feng, L. H. Xie, J. Zhang, M. Li, Y. B. Xie, J. R. Li and H. C. Zhou, *J. Am. Chem. Soc.*, 2016, **138**, 6204.

40 T. Ishiyama, M. Murata and N. Miyaura, *J. Org. Chem.*, 1995, **60**, 7508.

41 F. S. Han, *Chem. Soc. Rev.*, 2013, **42**, 5270.

42 A. S. Castanet, F. Colobert, P. E. Broutin and M. Obringer, *Tetrahedron: Asymmetry*, 2002, **13**, 659.

43 L. Grimaud and A. Jutand, *Synthesis*, 2017, **49**, 1182.